Modeling the impacts of COVID-19 mobility disruptions on respiratory syncytial virus (RSV) epidemics in a large metropolitan county

Complexity72h

Atchuta Srinivas Duddu [*1], Islam Elgamal [†2], Jose Camacho-Mateu[‡3], Olena Holubowska [§4], Simon Rella [¶5], Giulia Pullano [‖6], and Amanda C. Perofsky [**7,8]

[1]Department of Bioengineering, Indian Institute of Science, Bangalore, India
[2]Department of Scientific Computing, Technical University of Munich, Germany
[3]Department of Mathematics, Universidad Carlos III, Madrid, Spain
[4]Department of Earth and Environmental Sciences, KU Leuven University, Leuven, Belgium
[5]Institute of Science and Technology, Klosterneuburg, Austria
[6]Biology Department, Georgetown University, Washington, DC, USA
[7]Brotman Baty Institute for Precision, University of Washington, Seattle, Washington, USA
[8]Fogarty International Center, National Institutes of Health, Bethesda, Maryland, USA

June 28, 2024

Abstract

Background: Respiratory Syncytial Virus (RSV) infection is a major cause of acute respiratory hospitalizations in young children and older adults. In early 2020 RSV circulation declined dramatically at a global scale due to COVID-19 public health measures. Reductions in contacts and masking mandates disrupted the typical seasonality of RSV, with many locations not experiencing RSV recirculation until late 2020 or 2021. Here we use a mechanistic transmission model incorporating human mobility to project the rebound of RSV in Seattle-King County, Washington, USA.
Methods: We characterized within-city mixing, in-flows, and foot traffic to points of interest using mobility data from SafeGraph. We fit an age-structured predictive epidemiological model to RSV hospitalizations from January 2017 to January 2023, allowing for reductions in transmission due to changes in population behavior during the pandemic. We apply the model to project the first two waves of RSV rebound and assess which aspects of human behavior may be most relevant for predicting RSV reemergence.
Results: The inverse shortest path in the mobility network and inflow of visitors from Washington counties best capture the two-wave rebound pattern. Other mobility indicators, such as within neighborhood movement and child day care visits, produced inaccurate projections of RSV spread. Those results show how different indicators may affect the accuracy of the model, and the

Keywords Human Mobility · RSV · Mechanistic Model

*atchutaduddu@iisc.ac.in
†i.elgamal@tum.de
‡joscamac@math.uc3m.es
§olena.holubowska@kuleuven.be
¶simon.rella@ista.ac.at
‖giulia.pullano@georgetown.edu
**acperof@uw.edu

1 Introduction

In early 2020, most countries implemented Non-Pharmaceutical Interventions (NPIs) to reduce the spread of SARS-CoV-2, such as stay-at-home orders, gathering restrictions, travel bans, and school and business closures (Prem et al. [2020], Chinazzi et al. [2020]). These physical distancing measures, combined with face mask mandates, caused dramatic declines in other respiratory pathogens.

A significant correlation has been observed globally between reduced mobility and decreased transmissibility of the SARS-CoV-2 virus Nouvellet et al. [2021]. However, this relationship has evolved over time and varied across different countries, reflecting the introduction of new interventions, the rollout of vaccination programs, and cultural differences Sorokowska et al. [2017].

The relation between mobility and infection was found to be non-uniform, influenced by the timing and nature of interventions in each region Nouvellet et al. [2021]. This dynamic interplay underscores the complexity of managing a global pandemic, where local contexts and responses significantly impact outcomes Mellan et al. [2020], Vollmer et al. [2020].

Importantly, the implementation of NPIs for SARS-CoV-2 has had comparable effects on directly transmitted endemic diseases, including RSV Baker et al. [2020], Zheng et al. [2021a], which causes severe lower respiratory infections in infants and the elderly (Haynes et al. [2014]). RSV predominantly affects low- and middle-income countries and is estimated to account for 5% of mortality in children under five years old. Infants under six months are at the highest risk, but significant infection rates are also observed in children up to two years old. While reinfection can occur at older ages due to the short waning time of RSV-specific antibodies, it rarely results in hospitalization.

The spread of RSV is influenced by movement patterns and seasonal climate variations, leading to an annual periodicity in case numbers (Pitzer et al. [2015], Waris and White [2006]). One of the main drives of the transmission is the contact between young children in the school context Zheng et al. [2021b] due to the high inter-group exposure. The SARS-CoV-2 pandemic altered the normal RSV seasonality globally, causing unusually low transmission rates during periods of strict NPIs. When these interventions were relaxed, many countries saw substantial outbreaks outside the typical RSV season (Bents et al. [2023],Pletz et al. [2022], Martinez et al. [2022], Löwensteyn et al. [2023]). Therefore, it is crucial to understand the dynamics of RSV during and after the Sars-CoV-2 pandemic. This understanding will aid in managing the spread, predicting future cases, and preparing hospitals for potential surges.

Current models rarely include mobility data that has been shown relevant (Perofsky et al. [2024], **?**], Pullano et al. [2021]). Mobility patterns, however, can be quantified in various ways. In this study, we assess various mobility measures to enhance the accuracy of hospitalization predictions in the Seattle area. To that end we employ a deterministic MSIRS compartmental model capable of predicting typical RSV cases and seasonality previous to the SARS-CoV-2 pandemic (Hogan et al. [2017], Pitzer et al. [2015]). We then incorporate the effect of different mobility indicators, such as within-city mixing, into this model and evaluate the model's predictive capabilities.

2 Results

2.1 RSV Hospitalization Patterns

The first community acquired COVID-19 case in the United States was reported on February 28, 2020, in the greater Seattle metropolitan area. To slow the spread of SARS-CoV-2, Washington state declared a State of Emergency of February 29, 2020, closed schools in King County on March 12, and enacted statewide stay-at-home orders on March 23. King County also recommended that workplaces allow employees to work from home on March 4 and closed indoor dining and other "nonessential" businesses on March 16.

The transmission rates of all respiratory pathogens dropped dramatically after the State of Emergency, though RSV cases and hospitalizations were already declining prior to February 29 (Perofsky et al. [2024]). COVID-19 NPIs suppressed RSV circulation throughout 2020 to mid-2021 (Perofsky et al. [2024]). RSV hospitalizations resurged beginning in June 2021, outside of typical seasonal patterns (Figure 2), following increasing visitor inflow, within-city mixing, reduced masking, and the return to in-person learning for school students in April 2021 (Perofsky et al. [2024]). RSV hospitalizations continued to increase throughout Fall 2021 and rapidly declined in January 2021 (Figure 2), potentially due to increased physical distancing in response to the Omicron BA.1 wave in Seattle (Perofsky et al. [2024]).

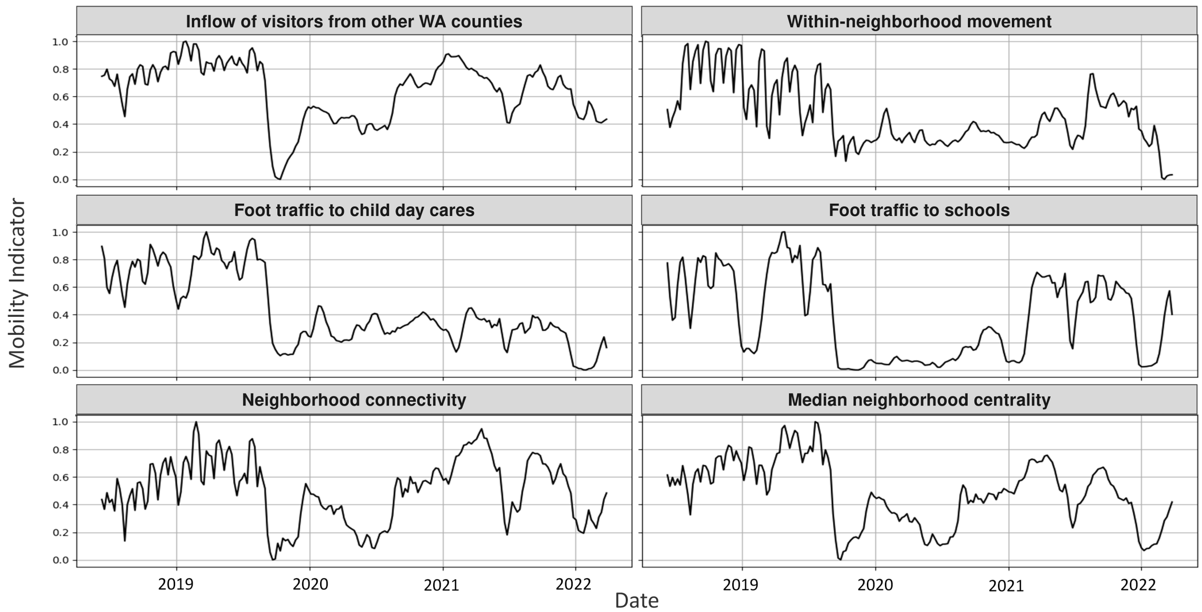

Figure 1: Mobility indicators in the greater Seattle region based on mobility network from aggregated mobile device location data, November 2018 – June 2022.

2.2 Disruptions to population mobility during the COVID-19 pandemic

We used aggregated mobile device location data for King County to approximate contact and movement patterns that are potentially relevant for RSV transmission. From November 2019 to March 2022, we estimated the weekly inflow of visitors residing in other Washington counties, within-neighborhood movement, foot traffic to elementary and high schools and child daycare centers, *neighborhood connectivity*, defined as the mean inverse shortest path length between neighborhoods in the mobility network, and neighborhood median weighted degree centrality, defined as the median degree of individual neighborhoods in the mobility network, based on the inflow of King County residents residing in other neighborhoods (Figure 1). Consistent with patterns observed for RSV hospitalizations, mobility declined substantially in early 2020, after the implementation of COVID-19 NPIs in King County. By the end of our mobility dataset in March 2022, within-neighborhood movement and foot traffic to child day cares were still below pre-pandemic levels, while the other mobility metrics gradually returned to pre-pandemic levels from the lifting of the stay-at-home restrictions in early June 2020 to early 2021 (Figure 1).

2.3 Modeling the impact of population mobility on RSV hospitalizations during the COVID-19 pandemic period, 2021 - 2023

We observed considerable variation across fits of the RSV transmission model to weekly hospitalizations during the pandemic period, depending on the particular mobility metric incorporated into the model. Neighborhood connectivity (the average inverse shortest path length among nodes in the mobility network) best estimated the timing and magnitude of two waves of RSV hospitalizations, although it underestimated the size of the first wave and overestimated the size of the second wave (Figure 2). The inflow of visitors from other counties in Washington, foot traffic to schools, and median neighborhood degree centrality captured the general timing of the two waves and the size of the first wave, but estimated a gradual increase in RSV hospitalizations after the first wave, instead of a defined second wave of hospitalizations beginning in Fall 2022 (Figure 2). Lastly, within-neighborhood movement and foot traffic to child day cares missed the first rebound of RSV hospitalizations and overestimated the second wave of hospitalizations (Figure 2).

We used the Akaike Information Criterion (AIC) (Akaike [1987]) to compare the fits of models to observed hospitalizations. The model incorporating neighborhood connectivity had the best fit to the data (lowest AIC score), followed by model including inflow of visitors from other Washington counties (Table 1). Models including the remaining mobility indicators had relatively poor fits to the data (Table 1).

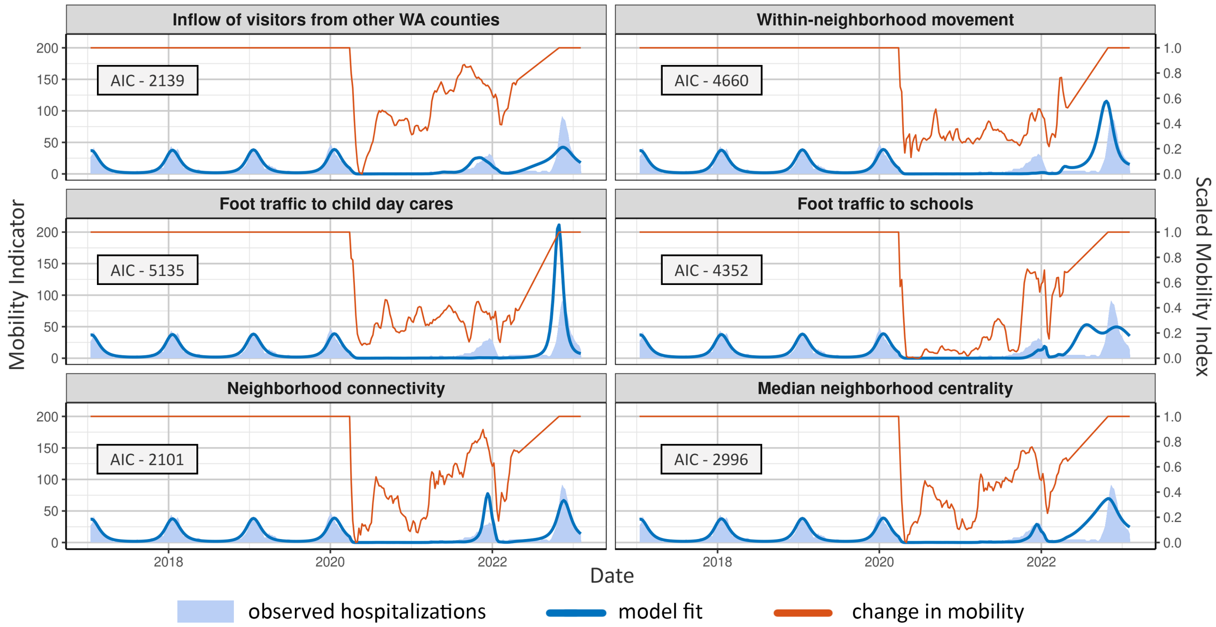

Figure 2: Model performance and fit of simulated RSV hospitalizations to actual hospitalization data in Seattle utilizing six different mobility indicators: Within State Movement, Within Neighborhood Movement, Child Day Care, Primary and Secondary Schools, Average Inverse Shortest Path and Median Node Strength.

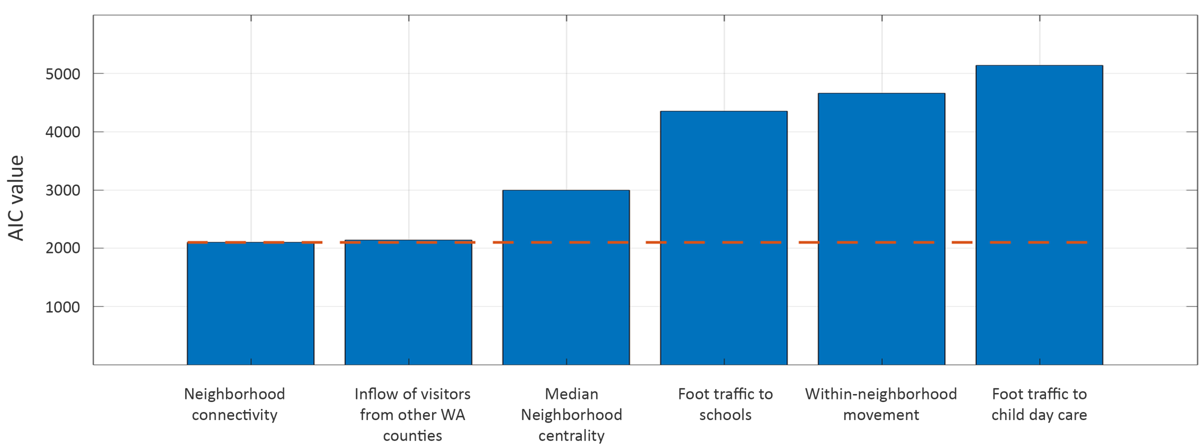

Figure 3: Comparison of AIC values for models using different mobility indicators: *Inflow of visitors from other WA counties*, *within-neighborhood movement*, *foot traffic to child day cares*, *foot traffic to schools*, *neighborhood connectivity*, defined as the average inverse shortest path length in the weighted mobility network, and *median neighborhood centrality*, defined as the median weighted node degree within the mobility network.

Model	AIC	ΔAIC
Neighborhood connectivity	2101	0
Inflow of visitors from other WA counties	2139	38
Median neighborhood centrality	2996	895
Foot traffic to schools	4352	2251
Within-neighborhood movement	4660	2559
Foot traffic to child day cares	5135	3034

Table 1: Comparison of model fits with AIC values.

3 Discussion

COVID-19 pandemic NPIs had profound effects on the transmission dynamics of various infectious diseases, including Respiratory Syncytial Virus (RSV). Our study examined the impact of mobility patterns on RSV transmission and subsequent hospitalizations in the greater Seattle area. By utilizing a deterministic compartmental model informed by mobility data, we were able to predict typical RSV hospitalizations and seasonality prior to the COVID-19 pandemic and compare these predictions with actual hospitalization data.

Our findings reveal that the utilization of mobility data metrics as indicators for the frequency of contacts and movements in a large metropolitan area produces accurate fits to the spread of RSV. The inverse shortest path in the mobility network and inflow of visitors from Washington counties best explain the two-wave profile of RSV hospitalizations after the lifting of social distancing measures. Epidemiological models including these indicators captured the peak timing of the two waves, suggesting that these factors are key in shaping RSV hospitalizations.

Surprisingly, points of interest related to the movements of children, such as foot traffic to daycares and primary and secondary schools, failed to accurately estimate RSV hospitalizations. This suggests that, while children have comparatively greater rates of infectiousness and high susceptibility to RSV than adults, their mobility alone cannot account for the timing or magnitude of RSV reemergence during the pandemic. Further research is needed into the relationship of mobility to points of interest that may be relevant to RSV transmission.

The study highlights the importance of considering mobility patterns in managing RSV and similar respiratory infections. The insights gained from this research can inform public health strategies, particularly in anticipating and mitigating the impacts of future changes in mobility. Furthermore, the ability to predict mobility patterns is critical in projecting RSV hospitalized cases.

We did not have mobility data corresponding to the time period of the second wave of RSV hospitalizations, and thus were unable to consider the impact of population behavior on this wave. We are unable to fit models to the season during the 2023-2024 season, after the second wave ending in March 2023, because of the availability of RSV vaccines and the RSV monoclonal antibody Nirsevimab introduce complexities not included in our model. Additionally, the future course of ongoing epidemics is highly sensitive to parameter values, making predictions from epidemiological models reliable only within a narrow time window and best interpreted in probabilistic terms.

Future research should continue to explore the effects of pandemic-related behavioral changes on the epidemiology of respiratory viruses. Additionally, incorporating real-time mobility and environmental conditions into predictive models could enhance our ability to forecast and control outbreaks, ultimately improving public health outcomes.

4 Methods

The creation of mobility metrics, network analyses, and RSV transmission modeling were performed using R version X and Python version 3.11.

4.1 Mobile Device Location Data and Calculation of Mobility Metrics

We obtained mobile device location data from SafeGraph (https://safegraph.com/), a data company that aggregates anonymized location data from 40 million devices, or approximately 10% of the United States population, to measure foot traffic to over 6 million physical places (points of interest) in the United States. From November 2019 to May 2022, we estimated weekly volume of foot traffic to specific points of interests (POIs), movement within and between census tracts, and the in-flow of visitors residing outside of King County, Washington, using SafeGraph's "Weekly Patterns" dataset, which provides weekly counts of the total number of unique devices visiting a POI from a particular home location. POIs are fixed locations, such as businesses or attractions. A "visit" indicates that a device entered the building or spatial perimeter designated as a POI. A "home location" of a device is defined as its common nighttime (18:00-7:00) census block group (CBG) for the past 6 consecutive weeks. We restricted our datasets to King County POIs that had been recorded in SafeGraph's dataset since January 2019. SafeGraph data were imported and processed using the SafeGraphR package (Huntington-Klein [2024]).

Following Perofsky et al. [2024], we measured movement within and between census tracts ("neighborhoods") in King County by extracting the home census tract of devices visiting points of interest (POIs) and limiting the dataset to devices with home locations in census tract of a given POI (within-neighborhood movement) or with home locations in census tracts outside of a given POI's census tract (between-neighborhood movement). To measure the inflow of visitors from other counties in Washington state or from out-of-state, we limited the dataset to devices visiting POIs in King County with home locations in other WA counties or in other US states, respectively. To measure foot traffic to specific categories of POIs, we aggregated daily visits to POIs by North American Industry Classification System (NAICS) category, without considering the home locations of devices visiting these POIs. To adjust for variation in SafeGraph's device panel size over time, we divided King County's census population size by the number of devices in SafeGraph's panel with home locations in King County each month and multiplied the number of weekly visitors by that value. For each mobility indicator, we summed adjusted weekly visits across POIs to generate county-level mobility indicators.

4.2 Weekly Mobility Networks, Node Degree Centrality, and Path Lengths

We used weekly movement of devices between census tracts to create weekly directed mobility networks. The edge weights $w_{ji}(T)$ were calculated as the weekly number of adjusted trips between source node *i* and target node *j*.

We used the NetworkX Python package (Hagberg et al. [2008]) to calculate the weekly weighted degree centrality and shortest path length among all nodes (census tracts) in the Seattle mobility network. Weighted degree centrality is the sum of the edge weights for edges incident to each node. For each week, we calculated the median weighted degree centrality among all nodes in the network. To measure path lengths in the network, we consider two nodes to be close together when there is a large flow of devices between them. We define the distance of each link between nodes as the inverse weight along the edge $l_{ji} = 1/w_{ji}$. We calculated the shortest path length L_{ji} between each pair of source node *i* and target node *j* using Dijkstra's algorithm (Dijkstra [1959]). Following Schlosser et al. [2020], we calculated the average path lengths among all nodes in the network each week as

$$L(T) = (n(n-1))^{-1} \sum_{i,j=1}^{n} C_i(T) \tag{1}$$

We then inverted the median path length $m(T) = 1/L(T)$ to estimate "network connectivity" in each week, with high values corresponding to overall shorter distances between nodes in the network.

4.3 Hospitalization Data

Weekly hospital visits diagnosed with RSV in King County, Washington, from January 2017 to November 2023, were provided by the Rapid Health Information Network (RHINO) program at the Washington Department of Health. All hospital discharge records from community hospitals in King County are included in this dataset. For privacy reasons, weekly hospitalizations with counts between 1-9 were suppressed and re-interpolated. To reduce noise in the dataset, we applied a centered 3-week moving average to the time series of hospitalizations and rounded values to the nearest whole number.

4.4 Demographic Data

The initial population size for King County was obtained from 1980 US census data. We assumed the birth rate varied over time, according to data on the crude annual birth rate from 1980 to 2022. Following Pitzer et al. [2015], we assumed individuals age exponentially into the next age class, with the rate of aging equal to 1/(width of the age class). We divided the <1 year age class into six 2-month age groups to better capture aging in this vulnerable age group. The remaining population was divided into seven classes: 1 year old, 2-4 years, 5–9 years, 10–19 years, 20–39 years, 40–59-years, and 60+ years old. We adjusted the net rate of immigration/emigration and deaths to produce a rate of population growth and age structure similar to that observed in King County, between 1980 and 2022.

4.5 RSV Transmission Model

4.5.1 Model Structure

We developed an age-structured $MSIRS$ transmission model for RSV (Maternal Immunity - Susceptible - Infected - Recovered - Susceptible), adapted from Pitzer et al. [2015] and Zheng et al. [2021a], which assumes short-term maternal immunity, frequent reinfection throughout life, and a gradual build-up of partial immunity following infection. By convention, for a given compartment X, we denote age group as uppercase, X^a, and levels of increasing immunity as lowercase, X_i (Figure 4).
We assume infants are born with transplacentally-acquired antibodies against RSV infections from their mothers (M), which wanes exponentially with mean 3-4 months (Ochola et al. [2009]). As transplacentally-acquired protective antibodies wane, infants become completely susceptible to infection (S_0).
We assume a partial build-up of immunity: Following each infection (I_i), individuals gain partial immunity that lowers their susceptibility to subsequent infections and the duration and relative infectiousness of subsequent infections (White et al. [2005],White et al. [2007], Weber et al. [2001], Pitzer et al. [2015]). We assume that infants with maternal immunity have a risk of infection that is similar to that of individuals who have had at least three infections.
The force of infection is influenced by the total number of infected individuals I, seasonal forcing, age-specific contact rates c_{ak}, and their relative infectiousness ρ_i, as well as factors of seasonal forcing,

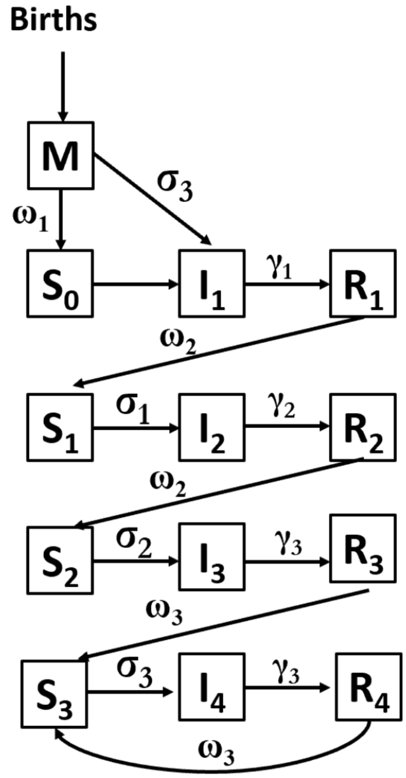

Figure 4: Overview of compartments in the MSIRS transmission model and their respective flows with rate parameters. M is the compartment of individuals with maternal immunity against RSV, S_i susceptible, I_i infected and R_i recovered individuals of immune maturity i. Hyperscript indices for age groups are omitted in this representation for clarity.

$$\lambda_a(t) = \sum_{k=1}^{13} \beta c_{ak}(1 + b\cos(2\pi(t-\phi))) \sum_{i=1}^{4} I_i^a \rho_i \quad , \tag{2}$$

where β is the baseline transmission rate of RSV, b is the amplitude of seasonal forcing and ϕ is the phase of seasonal forcing. Contacts among age groups are age-dependent and are given by the entries of contact matrix, c_{ak}. The rightmost sum is the product of infections with arbitrary immune maturity, I_i^a, scaled by their relative infectiousness ρ_i. Finally, a fraction Θ of infected individuals are hospitalized and reported,

$$H = \Theta \sum_{i=1}^{4} \sum_{a=1}^{13} I_k^a \quad . \tag{3}$$

In accordance with the available hospitalization data, we evaluate this model on a weekly basis, where a week corresponds to a time increment of roughly $1/52$ (a typical year has 52 weeks).
The used rate parameters are mostly taken from the literature and partly inferred from the available data of hospital-

Model Parameter	Value
Duration of infectiousness - first infection ($1/\gamma_1$)	10 days
Duration of infectiousness - second infection ($1/\gamma_2$)	7 days
Duration of infectiousness - third or later infection ($1/\gamma_3$)	5 days
Relative risk of infection following first infection (σ_1)	0.76
Relative risk of infection following second infection (σ_2)	0.6
Relative risk of infection following third or later infection (σ_3)	0.4
Relative risk of infection with maternal immunity (σ_3)	0.4
Relative risk of hospitalization given infection for M compartment	0.7
Duration of maternal immunity ($1/\omega_1$)	112 days
Duration of immunity following first and second infections ($1/\omega_2$)	182.625 days
Duration of immunity following third or later infections ($1/\omega_3$)	365.25 days
Relative infectiousness - second infection (ρ_1)	0.75
Relative infectiousness - third or later infections (ρ_2)	0.5
Baseline transmission rate (β)	Fitted
Amplitude of seasonal forcing (b)	Fitted
Phase of seasonal forcing (ϕ)	Fitted
Proportion of infections that lead to reported hospitalizations (Θ)	Fitted
Pandemic period mobility scalar μ	Fitted

Table 2: Parameters of the $MSIRS$ model taken from published literature or inferred from data during the model calibration process.

izations in the Seattle area between January 2017 and January 2023 (Table 2). The R package DeSolve was used for solving the MSIRS model.

4.5.2 Calibration Process

We use a two-step process to fit the pre-pandemic and pandemic periods. In the first step, we fit the core model described above to hospitalizations during the pre-pandemic period, January 2017 to March 2020. In the second step, we refit the model to a longer time series that includes the pandemic period, April 2020 to May 2023, keeping the same core parameters as in the first step but allowing for changes in population mobility to cause reductions in RSV transmission during the pandemic period.

In the first step, we used maximum likelihood estimation (MLE) to simultaneously fit the seasonal coefficients β, b, and ϕ and an infection-to-hospitalization scalar Θ to pre-pandemic hospitalizations. We note that Θ should not be interpreted as the true risk of hospitalization because estimates of RSV incidence typically focus on high-risk groups and not the general population. In the second step, we use hospitalizations during the pandemic period, April 2020 to May 2023, to estimate how COVID-19-related behavioral changes affected RSV transmission. We fit different time-varying mobility metrics, multiplied by a mobility scalar estimated by the model, to explore the impacts of different types of behavioral on RSV reemergence. We focused on mobility metrics that may best approximate contact and movement patterns that are relevant for RSV transmission. Specifically, we chose to test the impacts of weekly inflow of visitors residing in other Washington counties, within-neighborhood movement, foot traffic to elementary and high schools, foot traffic to child daycare centers, the mean inverse shortest path lengths between neighborhoods in the mobility network ("neighborhood connectivity"), and neighborhood median weighted degree centrality on RSV transmission.

5 Acknowledgements

This work is the output of the Complexity72h workshop, held at the Universidad Carlos III de Madrid in Leganés, Spain, 24-28 June 2024. https://www.complexity72h.com. We originally obtained RSV hospitalization data for work done in collaboration with Public Health - Seattle & King County: "Scenario Projections for Respiratory Syncytial Virus (RSV) Hospitalizations in the Context of New Immunizations, 2023-2024," for an initiative supported by the US Council of State and Territorial Epidemiologists (CSTE) and US Centers for Disease Control and Prevention (CDC): "Development of forecast, analytic, and visualization tools to improve outbreak response and support public health decision making." We also thank Daniela Paolotti for useful discussions about the design of the project.

References

Kiesha Prem, Yang Liu, Timothy W Russell, Adam J Kucharski, Rosalind M Eggo, Nicholas Davies, Stefan Flasche, Samuel Clifford, Carl AB Pearson, James D Munday, et al. The effect of control strategies to reduce social mixing on outcomes of the covid-19 epidemic in wuhan, china: a modelling study. *The Lancet Public Health*, 5(5):e261–e270, 2020.

Matteo Chinazzi, Jessica T Davis, Marco Ajelli, Corrado Gioannini, Maria Litvinova, Stefano Merler, Ana Pastore y Piontti, Kunpeng Mu, Luca Rossi, Kaiyuan Sun, et al. The effect of travel restrictions on the spread of the 2019 novel coronavirus (covid-19) outbreak. *Science*, 368(6489):395–400, 2020.

Pierre Nouvellet, Sangeeta Bhatia, Anne Cori, Kylie EC Ainslie, Marc Baguelin, Samir Bhatt, Adhiratha Boonyasiri, Nicholas F Brazeau, Lorenzo Cattarino, Laura V Cooper, et al. Reduction in mobility and covid-19 transmission. *Nature Communications*, 12(1):1–9, 2021.

Agnieszka Sorokowska, Piotr Sorokowski, Peter Hilpert, Katarzyna Cantarero, Tomasz Frackowiak, Khodabakhsh Ahmadi, Ahmad M Alghraibeh, Richmond Aryeetey, Anna Bertoni, Karim Bettache, et al. Preferred interpersonal distances: A global comparison. *Journal of Cross-Cultural Psychology*, 48(4):577–592, 2017.

Thomas A Mellan, Henrique H Hoeltgebaum, Swapnil Mishra, Charlie Whittaker, Ricardo P Schnekenberg, Axel Gandy, H Juliette T Unwin, Michaela AC Vollmer, Helen Coupland, Iwona Hawryluk, et al. Report 21: Estimating covid-19 cases and reproduction number in brazil. 2020.

Michaela AC Vollmer, Swapnil Mishra, H Juliette T Unwin, Axel Gandy, Thomas A Mellan, Valerie Bradley, Harrison Zhu, Helen Coupland, Iwona Hawryluk, Michael Hutchinson, et al. A sub-national analysis of the rate of transmission of covid-19 in italy. 2020.

Rachel E Baker, Sang Woo Park, Wenchang Yang, Gabriel A Vecchi, C Jessica E Metcalf, and Bryan T Grenfell. The impact of covid-19 nonpharmaceutical interventions on the future dynamics of endemic infections. *Proceedings of the National Academy of Sciences*, 117(48):30547–30553, 2020.

Zhe Zheng, Virginia E Pitzer, Eugene D Shapiro, Louis J Bont, and Daniel M Weinberger. Estimation of the timing and intensity of reemergence of respiratory syncytial virus following the covid-19 pandemic in the us. *JAMA Network Open*, 4(12):e2141779–e2141779, 2021a.

Amber K Haynes, Mila M Prill, Marika K Iwane, Susan I Gerber, Centers for Disease Control, Prevention (CDC), et al. Respiratory syncytial virus—united states, july 2012–june 2014. *MMWR Morb Mortal Wkly Rep*, 63(48):1133–1136, 2014.

Virginia E Pitzer, Cécile Viboud, Wladimir J Alonso, Tanya Wilcox, C Jessica Metcalf, Claudia A Steiner, Amber K Haynes, and Bryan T Grenfell. Environmental drivers of the spatiotemporal dynamics of respiratory syncytial virus in the united states. *PLoS Pathogens*, 11(1):e1004591, 2015.

Matti Waris and L White. Seasonality of respiratory syncytial virus infection. *Clinical Infectious Diseases*, 43(4), 2006.

Zhe Zheng, Virginia E Pitzer, Joshua L Warren, and Daniel M Weinberger. Community factors associated with local epidemic timing of respiratory syncytial virus: a spatiotemporal modeling study. *Science Advances*, 7(26):eabd6421, 2021b.

Samantha J Bents, Cécile Viboud, Bryan T Grenfell, Alexandra B Hogan, Stefano Tempia, Anne von Gottberg, Jocelyn Moyes, Sibongile Walaza, Chelsea Hansen, Cheryl Cohen, et al. Modeling the impact of covid-19 nonpharmaceutical interventions on respiratory syncytial virus transmission in south africa. *Influenza and Other Respiratory Viruses*, 17 (12):e13229, 2023.

Mathias W Pletz, Ralf Dürrwald, Janine Reiche, Norman Rose, André Scherag, and Sebastian Weis. Impact of the covid-19 pandemic on influenza and respiratory syncytial virus antibody titres in the community: a prospective cohort study in neustadt, thuringia, germany. *European Respiratory Journal*, 60(5), 2022.

Pamela P Martinez, Junya Li, Claudia P Cortes, Rachel E Baker, and Ayesha S Mahmud. The return of wintertime respiratory virus outbreaks and shifts in the age structure of incidence in the southern hemisphere. In *Open Forum Infectious Diseases*, volume 9, page ofac650. Oxford University Press US, 2022.

Yvette N Löwensteyn, Zhe Zheng, Neele Rave, Michiel AGE Bannier, Marie-Noëlle Billard, Jean-Sebastien Casalegno, Virginia E Pitzer, Joanne G Wildenbeest, Daniel M Weinberger, Louis Bont, et al. Year-round respiratory syncytial virus transmission in the netherlands following the covid-19 pandemic: A prospective nationwide observational and modeling study. *The Journal of Infectious Diseases*, 228(10):1394–1399, 2023.

Amanda C Perofsky, Chelsea L Hansen, Roy Burstein, Shanda Boyle, Robin Prentice, Cooper Marshall, David Reinhart, Ben Capodanno, Melissa Truong, Kristen Schwabe-Fry, et al. Impacts of human mobility on the citywide transmission dynamics of 18 respiratory viruses in pre-and post-covid-19 pandemic years. *Nature Communications*, 15(1):4164, 2024.

Giulia Pullano, Laura Di Domenico, Chiara E Sabbatini, Eugenio Valdano, Clément Turbelin, Marion Debin, Caroline Guerrisi, Charly Kengne-Kuetche, Cécile Souty, Thomas Hanslik, et al. Underdetection of cases of covid-19 in france threatens epidemic control. *Nature*, 590(7844):134–139, 2021.

Alexandra B Hogan, Patricia T Campbell, Christopher C Blyth, Faye J Lim, Parveen Fathima, Stephanie Davis, Hannah C Moore, and Kathryn Glass. Potential impact of a maternal vaccine for rsv: a mathematical modelling study. *Vaccine*, 35(45):6172–6179, 2017.

Hirotugu Akaike. Factor analysis and aic. *Psychometrika*, 52:317–332, 1987.

Nick Huntington-Klein. *SafeGraphR: Package for Processing and Analyzing SafeGraph Data*, 2024. URL `https://github.com/SafeGraphInc/SafeGraphR`. R package version 0.5.2.

Aric Hagberg, Pieter Swart, and Daniel S Chult. Exploring network structure, dynamics, and function using networkx. Technical report, Los Alamos National Lab.(LANL), Los Alamos, NM (United States), 2008.

Edsger W Dijkstra. A note on two problems in connexion with graphs. *Numerische Mathematik*, 1(1):269–271, 1959.

Frank Schlosser, Benjamin F Maier, Olivia Jack, David Hinrichs, Adrian Zachariae, and Dirk Brockmann. COVID-19 lockdown induces disease-mitigating structural changes in mobility networks. *Proceedings of the National Academy of Sciences U. S. A.*, 117(52):32883–32890, December 2020.

Rachel Ochola, Charles Sande, Gregory Fegan, Paul D. Scott, Graham F. Medley, Patricia A. Cane, and D. James Nokes. The level and duration of rsv-specific maternal igg in infants in kilifi kenya. *PLOS ONE*, 4(12):1–6, 12 2009. URL `https://doi.org/10.1371/journal.pone.0008088`.

L J White, M Waris, P A Cane, D J Nokes, and G F Medley. The transmission dynamics of groups a and B human respiratory syncytial virus (hRSV) in england & wales and finland: seasonality and cross-protection. *Epidemiology Infection*, 133(2):279–289, April 2005.

L J White, J N Mandl, M G M Gomes, A T Bodley-Tickell, P A Cane, P Perez-Brena, J C Aguilar, M M Siqueira, S A Portes, S M Straliotto, M Waris, D J Nokes, and G F Medley. Understanding the transmission dynamics of respiratory syncytial virus using multiple time series and nested models. *Math. Biosci.*, 209(1):222–239, September 2007.

Andreas Weber, Martin Weber, and Paul Milligan. Modeling epidemics caused by respiratory syncytial virus (rsv). *Mathematical Biosciences*, 172(2):95–113, 2001. ISSN 0025-5564. doi:https://doi.org/10.1016/S0025-5564(01)00066-9. URL `https://www.sciencedirect.com/science/article/pii/S0025556401000669`.